

# Dynamics and Free Energy of Polymers Partitioning into a Nanoscale Pore

Sergey M. Bezrukov,<sup>\*,†,‡</sup> Igor Vodyanoy,<sup>†,§</sup> Rafik A. Brutyan,<sup>†,⊥</sup> and John J. Kasianowicz<sup>\*,||</sup>

NIH, Division of Computer Research and Technology, 5/405, Bethesda, Maryland 20892, St. Petersburg Nuclear Physics Institute, Gatchina, 188350 Russia, ONR Europe, 223 Old Marylebone Road, London NW1 5TH, U.K., Institute of Biotechnology, Yerevan, Armenia 375056, and NIST, Biotechnology Division, 222/A353, Gaithersburg, Maryland 20899

Received June 10, 1996; Revised Manuscript Received September 20, 1996<sup>®</sup>

**ABSTRACT:** Membrane-bound proteinaceous nanoscale pores allow us to simultaneously observe the thermodynamic and kinetic properties of differently sized polymers within their confines. We determine the dynamic partitioning of poly(ethylene glycol) (PEG) into the pore formed by *Staphylococcus aureus*  $\alpha$ -toxin and evaluate the free energy of polymer confinement by measuring polymer-induced changes to the pore's ionic conductance. The free energy deduced from the partition coefficient has a sharper dependence on polymer length (or weight) than scaling theory predicts. Moreover, the polymer-induced conductance fluctuations show a striking nonmonotonic dependence on the polymer molecular weight. The movement of polymer inside the pore is characterized by a diffusion coefficient that is orders of magnitude smaller than that for polymer in the bulk aqueous solution, which suggests that PEG has an attractive interaction with the pore. Using an ad-hoc approach, we show that a simple molecular weight-dependent modification of the polymer's diffusion coefficient accounts for these results, but only qualitatively. Given that PEG associates with hydrophobic regions in proteins, we also conclude that, contrary to the conventional view of ion channels, the aqueous cavity of the  $\alpha$ -toxin pore's interior is, to some extent, hydrophobic.

## Introduction

Besides the well-known industrial applications for water-soluble polymers,<sup>1</sup> nonelectrolyte linear polymers are playing an increasingly important role in biomedical technology, in part because of their newly found ability to render surfaces relatively inert to attack from the immune system.<sup>2</sup> Since water-soluble polymers also generate well-defined osmotic pressures, they are used extensively in studies of the hydration properties of macromolecules<sup>3</sup> and the intermolecular forces between macromolecular assemblies.<sup>4</sup> These polymers, which include poly(ethylene glycol) (PEG), dextran, and poly(vinyl pyrrolidone), were recently used to estimate the physical properties of protein ion conducting pores, including their access resistance,<sup>5</sup> their radii,<sup>6,7</sup> and the change in the pore volume upon "gating" between different conductance states.<sup>8</sup> In such studies, it is implicitly assumed that the polymers do not directly interact with the pore. We present evidence below that this assumption is not always valid.

Given the extensive use of flexible water-soluble polymers in industry, biotechnology, and research, the physics that describes their equilibrium, kinetic, and transport properties is clearly important. Polymer science has already provided insight into how proteins fold into their three-dimensional structures,<sup>9</sup> but a clearer picture of the relative importance of site-specific interactions versus kinetic and entropic factors is still needed. Numerous studies of polymer transport through well-defined nucleopore filters were performed in which the effects of restricted diffusion were reported for both

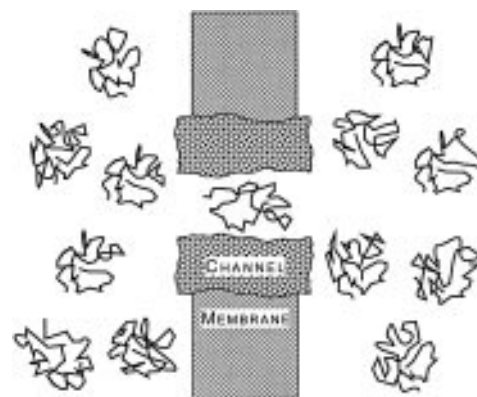


**Figure 1.** Schematic illustration of the  $\alpha$ -toxin pore in the presence of penetrating polymer chains. The nonelectrolyte polymers in the bulk aqueous phase are in dynamic equilibrium with those in the pore's interior. PEG entry into the pore will change the pore's conductance, thus signaling the polymer's presence.

branched and linear polymers.<sup>10</sup> However, these experiments do not clearly discriminate between the ability of the polymer to partition into and diffuse within the pores. To characterize the dynamics of polymers within confined geometries, dynamic light scattering experiments were performed on porous glasses equilibrated with dilute and semidilute polymer solutions.<sup>11</sup> In these experiments, the geometry is complex, but it was still possible to obtain estimates of the apparent diffusion coefficients for polymers trapped in these pores by comparing the dynamics of the polymers in the bulk with those in the porous glass.

We demonstrate a new method to simultaneously study polymer partitioning into, and their dynamics within, a short, narrow pore (Figure 1) with dimensions that are at least an order of magnitude smaller than those previously studied.<sup>10,11</sup> Specifically, we measure, with high resolution, the ionic conductance of a pro-

<sup>†</sup> NIH.

<sup>‡</sup> St. Petersburg Nuclear Physics Institute.

<sup>§</sup> ONR Europe.

<sup>⊥</sup> Institute of Biotechnology.

<sup>||</sup> NIST.

<sup>®</sup> Abstract published in *Advance ACS Abstracts*, November 15, 1996.

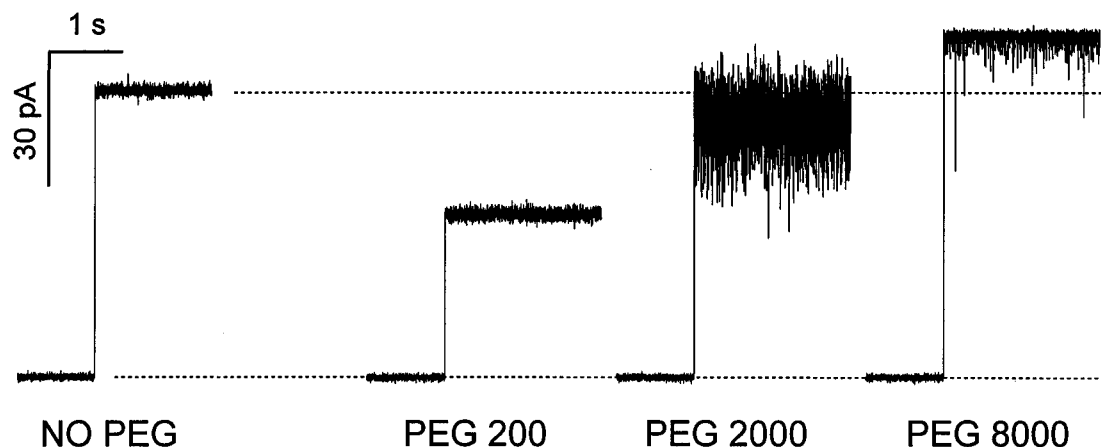


**Figure 2.** Effect of different molecular weight PEGs on the single  $\alpha$ -toxin pore current.<sup>15</sup> The leftmost trace illustrates the current jump caused by the spontaneous formation of a pore in the absence of polymer. The three recordings on the right show the influence of differently sized polymers on the open pore current. Low molecular weight PEGs penetrate the pore and cause a significant decrease in the mean pore conductance. Intermediately sized polymers cause a smaller decrease in the conductance but induce marked fluctuations. Note that the current noise is nonmonotonic in polymer molecular weight. Specifically, the noise track corresponding to the current through the pore in the presence of PEG 2000 is much wider than to those observed in the presence of higher and lower molecular weight polymer. The increase in the pore conductance caused by channel-impermeant PEG 8000 is discussed in the text. In all measurements, the concentration of polymer was 15% for all PEG molecular weights, and the applied potential was 100 mV. The signal was filtered with a low-pass Bessel filter at 1 kHz.

teinaceous channel in the presence of water-soluble polymers. In contrast with earlier work, we are able to observe the stochastic behavior of polymers confined in a *single* pore. Since the pore is small, the number of polymers in it is small, too, and the relative fluctuations around the average are large and thus easily observable.

We report here measurements of polymer-induced changes in current through single pores formed by *Staphylococcus aureus*  $\alpha$ -toxin<sup>12</sup> reconstituted into planar lipid bilayer membranes. This pore is well suited for studying polymer-pore interactions, because it can remain fully open for extended periods of time.<sup>13</sup> We show that the polymer-induced changes to the mean current and the current fluctuations permit the evaluation of the polymer partition coefficient and the polymer dynamics within the pore. The results suggest that PEG interacts with this pore to such an extent that it might be lined with hydrophobic residues. Thus, polymers provide us with a new tool to probe the details of a pore's interior. It is also conceivable that these pores should prove useful in obtaining additional information about the physical properties of polymers within confined geometries.

## Experimental Section

We characterize the interaction of polymers with a single protein pore that spans a lipid bilayer membrane. Specifically, we measured the ionic current that flows through a pore with a fixed applied potential,  $V = 100$  mV, in the presence of differently sized polymers. The pores were formed by adding less than 1  $\mu$ g of  $\alpha$ -toxin to one side of a planar lipid bilayer membrane,<sup>13,14</sup> which was bathed by symmetric aqueous solutions containing 1 M NaCl, 2.5 mM MES (or HEPES) at pH 7.5. Fifteen percent (w/w) of a given molecular weight PEG or dextran was added to the salt solution. We used PEGs with molecular weights between 200 and 17 000 (Aldrich, Milwaukee, WI, and Fluka, Buchs, Switzerland) and dextrans with molecular weights between 15 000 and 20 000 (Aldrich). PEG 1540 was specified by the manufacturer to have  $M_n = 1300$ –1600. Solvent-free membranes were formed from diphytanoyl phosphatidylcholine (Avanti Polar Lipids, Inc., Alabaster, AL) in high-purity pentane (Burdick and Jackson, Muskegon, MI), and the current was measured and analyzed as described earlier.<sup>13</sup> The temperature was  $T = (24.0 \pm 1.5)^\circ\text{C}$ .

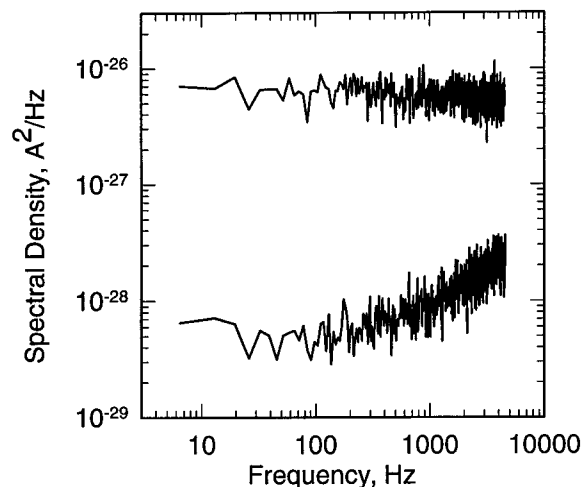
## Results and Discussion

Figure 2 illustrates the current through the open pore in the presence and absence of PEG in the membrane-bathing solution. It shows that the current through a single pore varies with PEG molecular weight in two ways. First, the mean current increases with increasing polymer weight. Second, there is also a marked and nonmonotonic difference in the current noise of the pore's open state, depending on the polymer molecular weight. The noise track corresponding to the current through the pore in the presence of PEG 2000 is much wider compared to that in the presence of higher and lower molecular weight polymer.

To quantify the intensity of polymer-induced current noise, we use power spectrum analysis,<sup>16</sup> which facilitates the decomposition of a noise signal from different sources. This statistical method gives the frequency content of the mean square fluctuation. Figure 3 illustrates the current spectral density for a single  $\alpha$ -toxin pore in the presence of PEG 1000 (top trace) versus the background in the absence of a pore (bottom trace).

The spectral density averaged over the frequency range between 100 and 1000 Hz for a variety of polymer molecular weights is illustrated in Figure 4. Note that the low-frequency noise is reduced at the extremes of PEG molecular weight and reaches a sharp peak for PEG 2000.<sup>17</sup> This distinct peak *cannot* be explained by assuming that PEG merely diffuses through the pore and suggests that PEG has an attractive interaction with the pore wall, perhaps reversibly adsorbing to the pore wall (see below). To further demonstrate that the polymer and pore interact, we show that a simple diffusion model for the polymer in the pore does not describe the results in Figure 4 (dotted-dashed and dashed lines), even if corrections for restricted diffusion<sup>10,11,18</sup> are included (see below).

Steady-state measurements of the pore conductance provide further evidence for a PEG-pore interaction. PEGs added to the bulk aqueous phase decrease the bulk conductivity approximately linearly with polymer concentration for  $[\text{PEG}] < 15\%$  (w/w) (data not shown). Polymers that partition into the pore should similarly



**Figure 3.** Power spectral density of the current through a single  $\alpha$ -toxin pore in the presence of PEG 1000 (top trace) vs the background in the absence of a pore (bottom trace). Note that the spectral density is "white" at these frequencies. The spectral density averaged over the range  $100 < f < 1000$  Hz, for a variety of differently sized PEGs, is illustrated in Figure 4.

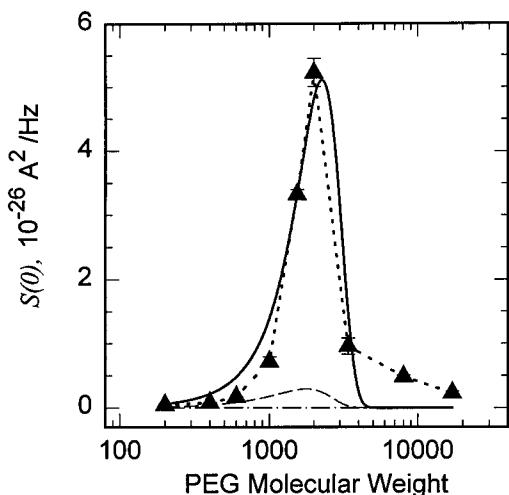


**Figure 4.** Low-frequency spectral density,  $S(0)$ , as a function of PEG molecular weight. The noise reaches a sharp peak at PEG 2000 and declines by more than a factor of 4 when the polymer mass is increased or decreased by a factor of 2. The dotted line through the points is drawn only to guide the eye. This distinct peak sharpness and the magnitude of the current noise *cannot* be explained by assuming that PEG merely diffuses through the pore, as is illustrated, using eq 8, by the dotted-dashed line ( $D = D_{\text{bulk}}$ ) or the dashed line ( $D = D_{\text{bulk}}/100$ ). Thus, PEG is probably attracted to the pore wall. This notion is further supported by the excessive reduction of the pore conductance caused by small polymers (Figure 5). The solid line is the result of a least-squares fit to an ad-hoc model for a polymer weight-dependent diffusion coefficient (see below).

cause a decrease in the conductance. They do. Figure 5 shows the relative change in the conductance as a function of PEG molecular weight ( $\blacklozenge$ ). Three features are clearly seen. First, PEGs with MW  $< 3400$  partition into the pore and decrease the pore's conductance. Second, higher molecular weight PEGs, which apparently do not partition into the pore, increase the conductance. The latter effect is caused by the water binding properties of PEG, which increases the electrolyte activity.<sup>5</sup> Third, the lowest molecular weight PEGs (MW  $< 1000$ ) decrease the pore conductance more effectively than they do the bulk solution conductivity

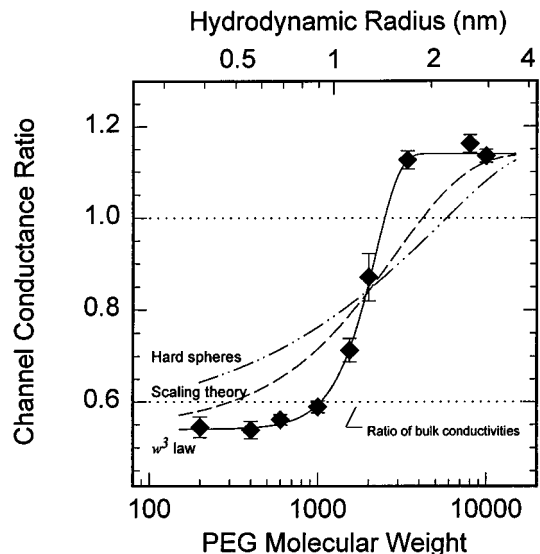


**Figure 5.** Relative change in the single pore conductance as a function of PEG molecular weight. The conductance *increases* in the presence of pore-impermeant PEGs (MW  $> 3400$ ) due to PEG's effect on the electrolyte activity. For PEG  $\leq 1000$  MW, the conductance ratio is *less* than that measured for the ratio of bulk conductivities, which may suggest that PEG monomers are attracted by the walls of the pore. The solid line is drawn according to eq 3, where the partition coefficient is  $p(w) = e^{-(w/w_0)^3}$  and  $w_0 = 2200$ . The dashed line and dotted-dashed line are the best-fit predictions based on scaling theory<sup>21,22</sup> and the partitioning of hard spheres into a cylinder,<sup>20</sup> respectively. The values of the PEG hydrodynamic radii<sup>23</sup> are denoted on the top axis.

(compare the data with the horizontal dotted line near the bottom).

**Polymer Partition Coefficient.** To describe the data in Figure 5, we assume that polymers with molecular weight  $w$  partition into the pore, causing a decrease in the conductance,  $\Delta g(w)$ , that, for fixed monomer concentration in the bulk aqueous phase, can be written in the form

$$\Delta g(w) \propto p(w) \quad (1)$$

where  $p(w)$  is the ratio of the average monomer density inside the pore to that in the solution outside the pore. We assume that the partition coefficient  $p(w)$  can be described by

$$p(w) = e^{-(w/w_0)^\alpha} \quad (2)$$

where  $\alpha$  and  $w_0$  are adjustable parameters that we obtain from experiment. Note that the partition coefficient approaches a step function for large  $\alpha$  and varies smoothly with molecular weight for small  $\alpha$ .

We determine the partition coefficient by fitting eqs 1 and 2 to the polymer-induced changes in the single pore conductance in the form

$$g(w)/g_0 = \beta(1 - (1 - \sigma'/\beta\sigma)p(w)) \quad (3)$$

where  $g(w)$  and  $g_0$  are the pore conductances in the presence and absence of polymer, and  $\sigma'$ , and  $\sigma$  are the corresponding bulk conductivities. The parameter  $\beta = 1.14$  describes the increase in salt activity caused by PEG and is determined independently.<sup>5</sup>

The ratio of the bulk conductivities in the presence and absence of polymer is  $\sigma'/\sigma = 0.6$  (horizontal dotted line, bottom of Figure 5). However, for low molecular weight PEGs which partition completely into the pore,

$g(w)/g_0 = 0.54$ . This deviation may reflect a favorable interaction of PEG with the pore's interior, which leads to an increased polymer concentration inside the pore. However, it may also be caused by differences in the conductance mechanisms in the  $\alpha$ -toxin pore and in bulk solution.<sup>13,19</sup> Taking  $\sigma'/\sigma = 0.54$ , and fitting eq 3 to the data using the expression for the partition coefficient  $p(w)$  described by eq 2, we find that  $\alpha = 3.1 \pm 0.2$  and  $w_0 = 2200 \pm 100$  (solid line, Figure 5).

Fitting the data to theories developed either for the partitioning of hard spheres into a cylindrical pore<sup>20</sup> or on the basis of scaling arguments<sup>21,22</sup> (see below) demonstrates that neither approach describes the sharp dependence of the partitioning on polymer molecular weight.<sup>24</sup>

**Free Energy Estimate.** We report here measurements of polymer partitioning into a  $\sim 1.2$  nm radius proteinaceous pore in a planar lipid bilayer. It is important to note that this system is different from the idealized case developed by de Gennes for polymer chains with hydrodynamic radii much larger than the tube radius.<sup>21</sup> We observe pronounced changes in the pore conductance for polymer sizes that are approximately equal to the pore radius and, thus, are limited to this size range. Nevertheless, it is interesting to compare our results with the theoretical prediction based on scaling arguments. As is shown below, the scaling approach gives approximately the right polymer size, which corresponds to one  $kT$  in the free energy of partitioning, but predicts a much wider molecular weight transition range for the partition coefficient (dashed line, Figure 5) than we observe.

For a real chain in a good solvent, the free energy of confining it in a narrow cylinder is

$$F_{\text{conf}} \cong kTN(a/2r)^{5/3} \quad (4)$$

where  $N$  is the number of freely jointed chain segments,  $a$  is the segment length, and  $r$  is the tube radius.<sup>21,22</sup>

We first estimate the size of a coil which corresponds to one  $kT$  of the free energy of polymer confinement. To do this, we assume that the numerical coefficient omitted in the left hand side of eq 4 is close to 1. From eq 4, it follows, then, that the number of polymer segments entrapped in the pore in this case is

$$N = (a/2r)^{-5/3} \quad (5)$$

such that the average end-to-end distance for this energy is given by<sup>21</sup>

$$\langle R^2 \rangle^{1/2} \equiv aN^{3/5} = 2r \quad (6)$$

This result is in qualitative agreement with our data. Indeed, if we write the polymer-pore partition coefficient in the form

$$p(N) = e^{-F_{\text{conf}}(N)/kT} \quad (7)$$

then an e-fold reduction in polymer partitioning into the pore should occur at the free energy,  $F_{\text{conf}}(N)$ , equal to one  $kT$ , i.e., according to eq 6, at the molecular weight for which the polymer average end-to-end distance,  $\langle R^2 \rangle^{1/2}$ , and the pore diameter,  $2r$ , are equal. Since the hydrodynamic radius is given by<sup>22</sup>  $R_D \cong 0.271 \langle R^2 \rangle^{1/2}$ , from eq 6 we obtain  $r = 1.85R_D$ . The data in Figure 5 show that the e-fold reduction in the pore conductance caused by PEG occurs at polymer size  $R_D \cong 1.3$  nm; thus,  $r \cong 2.4$  nm.

**Pore Size.** The above estimate for the pore radius is about 2 times larger than that estimated from electron micrographs<sup>25</sup> or the pore's permeability to nonelectrolytes.<sup>7</sup> To size the  $\alpha$ -toxin pore independently, we did access resistance measurements<sup>5,26</sup> using pore-impermeant dextran of 15 000–20 000 MW. Dextran was added to the membrane-bathing solution while the pore's conductance was monitored. Fourteen percent dextran (w/w) increased the specific resistivity of bulk solution by  $\Delta\rho = 0.059 \Omega\cdot\text{m}$  and increased the pore's resistance by  $\Delta R = 26 \pm 5 \text{ M}\Omega$ . As a result, the pore radius, defined by<sup>26</sup>  $r = \Delta\rho/2\Delta R$ , is estimated to be  $r = 1.1 \pm 0.2$  nm, which is in good agreement with estimates based on other methods.

**Polymer-Pore Interaction.** The previous discussion shows that the characteristic "cutoff" polymer size deduced from the PEG partitioning measurements (Figure 5) is close to the value obtained as a result of the formal application of scaling theory<sup>21</sup> but shifted to higher molecular weights. This might indicate a favorable interaction between PEG and the surface of the pore, which partly compensates the loss in entropy for polymers penetrating into the pore. More evidence for this interpretation is supplied by the functional dependence of the partition coefficient on polymer weight, which is quite different from that predicted by theories which neglect such interactions. Experimentally, there is a much sharper dependence of PEG's partition coefficient on polymer size. Indeed, from eqs 4 and 7, it follows that the partition coefficient should be proportional to  $e^{-w/w_0}$ , not to  $e^{-(w/w_0)^3}$ , as we report here. Correspondingly, the free energy of polymer confinement deduced from the experiments is proportional to the cube of the number of polymer segments entrapped in the pore, in contrast to eq 4, which predicts a linear dependence on  $N$ . The interaction is also made manifest by the dependence of the current noise on polymer molecular weight (Figure 4). Specifically, it has a pronounced and well-defined peak at MW = 2000, which is in marked disagreement with the prediction of a free diffusion model<sup>18</sup> that is illustrated as the dotted-dashed and dashed lines in Figure 4. Thus, our results offer compelling evidence that the polymer partitions into the pore and is attracted to the pore's interior.

The introduction of a polymer-pore interaction that is proportional to the number of monomers per polymer qualitatively mimics the low-frequency noise behavior. Conductance fluctuations here are assumed to be generated by the random, diffusion-driven exchange of polymers between the membrane-bathing solution and the pore. If we assume that polymers do not interact with each other inside the pore, then the low-frequency current spectral density,<sup>18</sup>

$$S(0) = \Delta g_1(w)^2 V^2 \langle n(w) \rangle L^2 / 3D(w) \quad (8)$$

is expressed in terms of the reduction of the pore conductance caused by the entry of a single polymer into the pore,  $\Delta g_1(w)$ , the transmembrane potential difference,  $V$ , the average number of polymers in the pore,  $\langle n(w) \rangle$ , the pore length,  $L$ , and the diffusion coefficient of a polymer molecule inside the pore,  $D(w)$ . Here,  $\Delta g_1(w)^2 V^2 \langle n(w) \rangle$  represents the polymer-induced contribution to the root-mean-square current noise caused by the pore fluctuating between different conductance values corresponding to the entry and exit of polymers, and  $L^2/3D(w)$  is related to the effective correlation time for polymer egress from the pore.

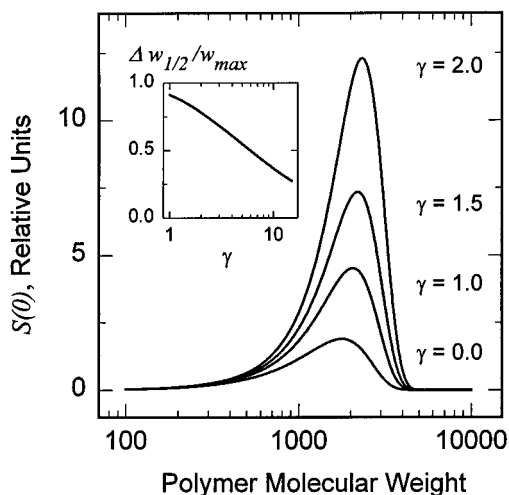


**Figure 6.** Dependence of the theoretically predicted low-frequency spectral density on polymer molecular weight. The parameter  $\gamma$  describes the degree of polymer–pore interaction in the particular model we use here (eq 10). The value of  $\gamma = 0$  corresponds to a free diffusion model.<sup>18</sup> Higher values of  $\gamma$  correspond to higher fluctuation levels and reduce the relative half-width ( $\Delta w_{1/2}/w_{\max}$ ) of the spectral density dependence on the polymer molecular weight (inset). Here,  $w_{\max}$  is the polymer molecular weight that causes the maximum intensity of low-frequency current noise.

Assuming that  $\Delta g_i(w)$  is proportional to the number of monomers in the polymer chain and that the diffusion coefficient scales as the inverse chain hydrodynamic radius in free solution, we have

$$S(0) \propto w^{8/5} p(w) \quad (9)$$

Figure 6 illustrates this dependence using the partition coefficient obtained from pore conductance as described above. Note that the diffusion model gives a nonmonotonic behavior of the low-frequency spectral density with a *smooth* maximum for polymer weights around 1500–2000, giving a slightly higher intensity at PEG 1540 (bottom curve). This is in striking contrast to the results illustrated in Figure 4. The dependence of the experimental current noise on PEG molecular weight has a different shape, exhibiting a sharp peak at MW = 2000. Moreover, the measured low-frequency noise for polymer molecular weights in the range of 1500–3400 is orders of magnitude higher than the noise predicted from the model if the diffusion coefficient,  $D(w)$ , is chosen to be anything close to its value in free solution (dotted-dashed line, Figure 4).

**Ad-Hoc Model For Interaction.** Introducing a polymer size-dependent interaction captures the essential features of the low-frequency noise. Suppose that the movement of a polymer inside the pore can be described by a molecular weight (i.e., polymer length)-dependent activation process (characterized by a parameter,  $\gamma$ ), such that the effective diffusion coefficient may be written as

$$D(w) \propto e^{-(\gamma w/w_0)/R_D} \quad (10)$$

Substituting this expression for the diffusion coefficient in eq 8, we calculate the relative low-frequency spectral density for different values of the dimensionless parameter  $\gamma$ , and we illustrate the results in Figure 6. The case  $\gamma = 0$ , the free diffusion model, is described by eq 9. Increasing  $\gamma$  sharpens the curve and increases the low-frequency noise, thus reproducing, though only

qualitatively, the features of the experimentally determined noise data in Figure 4. For example, the solid line in Figure 4 is the least-squares fit to the data with  $\gamma = 1.74$ . Note that the model curve describes the sharpness of the noise peak but fails at high molecular weights.

### Summary

We demonstrated that the statistical analysis of ion currents through a nanoscale proteinaceous pore in the presence of flexible linear polymers can be used to study the polymer's thermodynamic and kinetic properties. The free energy of polymer confinement in the pore deduced from our analysis differs significantly from predictions of scaling theory. The scaling approach yields a much weaker dependence of partitioning on the polymer molecular weight but, surprisingly, gives a correct estimate for the polymer size corresponding to one  $kT$  of energy. The characteristic size determined in this manner distinguishes between polymers that partition into and those that are entropically excluded from the pore.

Our results also suggest that PEG has an attractive interaction with the pore. This is in striking contrast to what one would expect if the pore is lined exclusively with hydrophilic amino acids. Recent work suggests that PEGs are excluded from proteins in their native conformation yet can associate with proteins in their denatured states.<sup>27</sup> Moreover, PEG appears to be excluded from hydrophilic regions of proteins and attracted to their hydrophobic segments.<sup>28</sup> Thus, the water-filled  $\alpha$ -toxin pore may, to some extent, be lined with hydrophobic residues. This challenges the conventional belief that an aqueous pore of an ion channel can contain only hydrophilic residues. If our conclusion is true, then the functional role of these residues is intriguing. One possible speculation is that they provide a mechanism to disrupt the water structure inside this pore to facilitate the transport of solutes.

Generally, questions of the structure–function relationship for ionic pores are addressed in terms of the pore's ability to conduct different ions.<sup>29</sup> Recently, evidence for a pore's role in the transmembrane transport of biopolymers, such as proteins, was obtained.<sup>30</sup> Here we have shown that a *simple* nonelectrolyte polymer can be used to probe a protein pore not only in terms of its physical size but also in terms of its functional properties. It is likely that different types of polymers will elicit characteristic channel–polymer interactions which are related, but not restricted, to polymer configuration limitations. In fact, the  $\alpha$ -toxin channel was recently used to detect and characterize individual molecules of single-stranded RNA and DNA.<sup>31</sup>

**Acknowledgment.** We thank Drs. V. A. Parsegian and D. C. Rau for stimulating discussions and critical comments and Dr. H. Bayley for the gift of  $\alpha$ -toxin. This work was supported in part by a National Academy of Sciences/National Research Council Research Associateship (J.J.K.) and by a grant from the ONR (V. A. Parsegian). Commercial names of materials and apparatus are identified only to specify the experimental procedure. This does not imply a recommendation, nor does it imply that they are the best available for the purpose.

### References and Notes

- (1) *Water-Soluble Polymers*, Shalaby, S. W., McCormick, C. L., Butler, G. B., Eds.; American Chemical Society: Washington, DC, 1991; p 350.

- (2) (a) Lasic, D.; Papahadjopoulos, D. *Science* **1994**, *267*, 1275. (b) Papahadjopoulos, D.; Allen, T. M.; Gabizon, A.; Mayhew, E.; Matthey, K.; Huang, S. K.; Lee, K. D.; Woodle, M. C.; Lasic, D. D.; Redemann, C.; Martin, F. J. *Proc. Natl. Acad. Sci. U.S.A.* **1991**, *88*, 11460.
- (3) Parsegian, V. A.; Rand, R. P.; Rau, D. C. *Methods Enzymol.* **1995**, *259*, 43.
- (4) Leikin, S. L.; Parsegian, V. A.; Rau, D. C.; Rand, R. P. *Annu. Rev. Phys. Chem.* **1993**, *44*, 369.
- (5) Bezrukov, S. M.; Vodyanoy, I. *Biophys. J.* **1993**, *64*, 16.
- (6) Colombini, M. *J. Membr. Biol.* **1980**, *53*, 79.
- (7) (a) Füssle, R.; Bhakdi, S.; Szegoleit, A.; Trantum-Jensen, J.; Kranz, T.; Wellensiek, H.-J. *J. Cell Biol.* **1981**, *91*, 83. (b) Krasilnikov, O. V.; Sabirov, R. Z.; Ternovsky, V. I.; Merzliak, P. G.; Muratkodjaev, J. N. *FEMS Microbiol. Immunol.* **1992**, *105*, 93. (c) Korchev, Y. E.; Bashford, C. L.; Alder, G. M.; Kasianowicz, J. J.; Pasternak, C. A. *J. Membr. Biol.* **1995**, *147*, 233.
- (8) (a) Zimmerberg, J.; Parsegian, V. A. *Nature* **1986**, *323*, 36; (b) Zimmerberg, J.; Bezanilla, F.; Parsegian, V. A. *Biophys. J.* **1990**, *57*, 1049; (c) Rayner, M. D.; Starkus, J. G.; Ruben, P. C.; Allcata, D. A. *Biophys. J.* **1992**, *61*, 96; (d) Vodyanoy, I.; Bezrukov, S. M.; Parsegian, V. A. *Biophys. J.* **1993**, *65*, 2097.
- (9) Srinivasan, R.; Rose, G. D. *Proteins Struct., Funct. Genet.* **1995**, *22*, 81.
- (10) (a) Davidson, M. G.; Deen, W. M. *Macromolecules* **1988**, *21*, 3474 and references therein. (b) Guillot, G. *Macromolecules* **1987**, *20*, 2600 and references therein.
- (11) (a) Teraoka, I.; Zhou, Z.; Langley, K. H.; Karasz, F. E. *Macromolecules* **1993**, *26*, 3223. (b) Teraoka, I.; Langley, K. H.; Karasz, F. E. *Macromolecules* **1993**, *26*, 287 and references therein.
- (12) (a) Menestrina, G. *J. Membr. Biol.* **1986**, *90*, 177. (b) Gouaux, J. E.; Braha, O.; Hobaugh, M. R.; Song, L.; Cheley, S.; Shustak, C.; Bayley, H. *Proc. Natl. Acad. Sci. U.S.A.* **1994**, *91*, 12828.
- (13) Kasianowicz, J. J.; Bezrukov, S. M. *Biophys. J.* **1995**, *69*, 94.
- (14) Montal, M.; Mueller, P. *Proc. Natl. Acad. Sci. U.S.A.* **1972**, *65*, 3561.
- (15) In the absence of PEG, the current noise is much lower<sup>13</sup> than in the presence of the polymer. For the purposes of this study, we ignore the fact that the current noise does not follow a Gaussian distribution about the mean current. This is especially evident at higher molecular weight polymers (e.g. PEG 8000). Amplitude histogram analysis provides additional information on the correlation time for PEG partitioning into the pore. The analysis will be provided in a forthcoming paper.
- (16) Neher, E.; Stevens, C. F. *Annu. Rev. Biophys. Bioeng.* **1977**, *6*, 345.
- (17) It is unlikely that the noise caused by PEG 2000 is the result of an anomaly of the surface-active properties of that particular polymer (see: Winterhalter, M.; Büchner, H.; Marzinka, S.; Benz, R.; Kasianowicz, J. J. *Biophys. J.* **1995**, *69*, 1372).
- (18) Bezrukov, S. M.; Vodyanoy, I.; Parsegian, V. A. *Nature (London)* **1994**, *370*, 279.
- (19) Bezrukov, S. M.; Kasianowicz, J. J. *Phys. Rev. Lett.* **1993**, *70*, 2352.
- (20) Colton, C. K.; Satterfield, C. N.; Lai, C.-J. *AIChE J.* **1975**, *21*, 289.
- (21) de Gennes, P.-G. *Scaling Concepts in Polymer Physics*; Cornell University Press: Ithaca, NY, 1979, p 46–53.
- (22) Grosberg, A. Yu.; Khokhlov, A. R. *Statistical Physics of Macromolecules*; AIP Press: New York, 1994.
- (23) Kuga, S. *J. Chromatogr.* **1981**, *206*, 449.
- (24) We obtain the free energy of polymer confinement directly from eq 7, neglecting contributions from the nonideal behavior of 15% PEG solutions. As deviations from Van't Hoff's law increase with increasing polymer size, larger polymers are pushed into the pore more so than smaller ones. Thus, the nonideality of PEG solutions should smoothen the transition between penetrating and excluded polymer sizes, which means that  $F_{\text{conf}}$  for more dilute polymer solutions should have an even *stronger* dependence on polymer weight than we report here.
- (25) Olofsson, A.; Kaveus, U.; Thelastam, M.; Hebert, H. *J. Ultrastruct. Res. Mol. Struct.* **1988**, *100*, 194.
- (26) Vodyanoy, I.; Bezrukov, S. M. *Biophys. J.* **1992**, *62*, 10.
- (27) Timasheff, S. N. *Annu. Rev. Biophys. Biomol. Struct.* **1993**, *22*, 67.
- (28) (a) Arakawa, T.; Timasheff, S. N. *Biochemistry* **1985**, *24*, 6756. (b) Lee, L.-Y.; Lee, J. C. *Biochemistry* **1987**, *26*, 7813. (c) Cleland, J. L.; Hedgepeth, C.; Wang, D. I. C. *J. Biol. Chem.* **1992**, *267*, 13327.
- (29) Hille, B. *Ionic channels of excitable membranes*, 2nd ed.; Sinauer Associates: Sunderland, MA, 1992.
- (30) (a) Simon, S. M.; Blobel, G. *Cell* **1991**, *65*, 371; **1992**, *69*, 677. (b) Bustamante, J. O.; Hanover, J. A.; Leipins, A. *J. Membr. Biol.* **1995**, *146*, 239. (c) Bustamante, J. O.; Oberleithner, H.; Hanover, J. A.; Leipins, A. *J. Membr. Biol.* **1995**, *146*, 253. (d) Bustamante, J. O.; Leipins, A.; Prendergast, R. A.; Hanover, J. A.; Oberleithner, H. *J. Membr. Biol.* **1995**, *146*, 263.
- (31) Kasianowicz, J. J.; Brandin, E.; Branton, D.; Deamer, D. W. *Proc. Natl. Acad. Sci. U.S.A.*, in press.

MA960841J